AIAA JOURNAL
Vol. 33, No. 2, February 1995

Aeroservoelastic Aspects of Wing/Control Surface Planform Shape Optimization

Eli Livne* and Wei-Lin Li†
University of Washington, Seattle, Washington 98195

Equivalent plate structural modeling and doublet point lifting surface unsteady aerodynamics are used to obtain analytic sensitivities of aeroelastic and aeroservoelastic response with respect to wing and control surface planform shape parameters. Rational function approximations for unsteady aerodynamic forces, their shape sensitivities, and the resulting linear time invariant state space models of aeroservoelastic systems and their shape sensitivities are examined. The goal is to develop effective and numerically efficient approximation techniques for wing shape optimization for use with nonlinear programming and approximation concepts as a multidisciplinary optimization strategy. Effects of structural and unsteady aerodynamic modeling errors are studied. Examination of approximation accuracy using alternative approximation techniques (and the resulting move limits) provide insight and experience on the way to realistic wing/control surface shape optimization with active controls and aeroservoelastic constraints.

Nomenclature

$[A(k, M_\infty)]$	= matrix of aerodynamic influence coefficients
b	= reference semichord
$[C]$	= damping matrix, viscous damping
$[E_j]$	= Roger approximation matrices
e_j	= elements of Roger approximation matrices for the i, j term of the generalized force matrix
$[G]$	= displacement feedback matrix
$\{\boldsymbol{H}_i\}, \{(\partial \boldsymbol{H}_i)/(\partial \boldsymbol{x})\}$	= slope and displacements due to motion in the ith generalized displacement
$\{\tilde{\boldsymbol{H}}_i\}$	= displacements at the pressure points due to motion in the ith generalized displacement
$H_i(x, y)$	= ith generalized displacement, mode shape
$\{\boldsymbol{h}^i\}, \{(\partial \boldsymbol{h}^i)/(\partial \boldsymbol{x})\}$	= vectors of displacements and slopes of deformation due to motion in mode i
$\hat{j}$	= pure imaginary number, $\sqrt{-1}$
$[K]$	= stiffness matrix
$K_{er}, [K_{er}]$	= kernel function and associated aerodynamic influence coefficient matrix
k	= reduced frequency
$[L]$	= coefficient matrix for least square Roger approximation process
$[M]$	= mass matrix
M_∞	= flight Mach number
m	= number of aerodynamic boxes
mi, ni	= powers of x and y, respectively, for the ith polynomial term
m_L	= number of lag roots in the Roger approximation
N_q	= number of generalized displacements
n_k	= number of reduced frequencies (excluding $k = 0$) used for Roger's approximation
p	= Laplace transform variable
$[Q]$	= generalized unsteady aerodynamic forces
Q_R, Q_I	= real and imaginary parts of the generalized aerodynamic force matrix
q_D	= dynamic pressure
$\{\boldsymbol{R}\}$	= right-hand-side vector in the Roger approximation equations for a single element ij of $[Q]$
$[T]$	= transformation matrix of displacements and rotations from structural to aerodynamic points
U	= true airspeed
$[U], [V]$	= matrices in the aeroservoelastic state space model, exact
$[\tilde{U}], [\tilde{V}]$	= approximated system matrices based on direct or reciprocal Taylor series expansions
$X_{CL}, X_{FR}, Y_{CL}, Y_{CR}, Y_R$	= coordinates defining control surface and wing tip locations, Fig. 1
$(\bar{x}, \bar{y})$	= coordinates of a point on the wing where displacement is measured for feedback purposes
x_i, y_i	= coordinates of the ith downwash point, 3/4 chord of the ith aerodynamic box in DPM
$\tilde{x}_i, \tilde{y}_i$	= coordinates of the ith pressure point, 1/4 chord on the ith aerodynamic box in DPM
β	= $\sqrt{m_\infty^2 - 1}$
β_l	= lag roots in the Roger approximation
Γ	= Feedback gain for displacement feedback
γ	= Euler's constant
$\{\Delta \boldsymbol{p}^j\}$	= vector of complex normalized pressures due to motion in generalized displacement j
$[\Delta S]$	= diagonal matrix of aerodynamic panel areas
σ_j	= width of jth aerodynamic strip

Received June 2, 1994; revision received Oct. 25, 1994; accepted for publication Oct. 25, 1994.

*Assistant Professor, Department of Aeronautics and Astronautics. Senior Member AIAA.

†Graduate Research Assistant, Department of Aeronautics and Astronautics.

Subscripts and Superscripts

c	= control surface rotation degrees of freedom
d	= downwash points
F	= full order
G	= gust input
h	= displacement
p	= pressure points
s	= structural degrees of freedom
α	= geometric angles of attack
$*$	= adjoint

Introduction

THE structural optimization of wings of given planforms subject to structural constraints as well as constraints on static and dynamic aeroelastic behavior has been extensively studied in the last 25 years.[1–3] Various design oriented modeling techniques have appeared. Behavior sensitivities for flutter, divergence, and control effectiveness constraints have been developed. Technology in this area has matured and has already made an impact on the design of real airplanes. During the preliminary design of airplanes, however, changes in wing planform should be allowed, either in the form of slight variations from a base configuration or as radical changes leading to different configurations.

The step from sizing type optimization (where the geometry is preassigned) to shape optimization, involving structural and aerodynamic interaction, leads to a major increase in the required computational resources. Challenges in the associated design oriented structural and aerodynamic modeling, as well as sensitivity analysis, effective approximations, and the integration of the disciplines have not yet been met satisfactorily, and the technology in this area is still evolving. Considerable progress in the area of wing shape optimization with static aeroelastic constraints has been made in recent years. Finite element structural models combined with vortex lattice aerodynamics[4,5] and equivalent plate structural models combined with aerodynamic strip and lifting surface theories[6,7] have been studied. Effective wing shape synthesis with classical flutter constraints, however, or effective wing shape design addressing aeroservoelastic interactions are still in their infancy.

Flutter and aeroservoelastic response present a serious challenge in terms of their demands on computer resources. Major difficulties arise, stemming from the need to carry out unsteady aerodynamic load calculations repetitively, generate efficient integrated aeroservoelastic models and evaluate aeroservoelastic stability and gust response time and again. Still, no integrated wing synthesis capability is complete without flutter and aeroservoelastic constraints.[8–11] As experience has shown, neglecting to consider aeroservoelastic interactions early in the design process can lead to serious problems and costly design fixes later. A research effort to develop techniques for effective aeroservoelastic optimization is currently underway but has mostly been limited to preassigned planforms.[12–15] As airplane design becomes more integrated, and structures, aerodynamics, and controls more coupled, the need to include aeroservoelastic constraints in the search for the best planform shape seems to become stronger. Flutter of single surfaces of varying shapes or due to interference between lifting surfaces,[16] stresses due to gusts with and without active load alleviation, and the best size and location of control surfaces for active control[17–19] all become important and should be addressed as early as possible. Currently, in the absence of a realistic integrated multidisciplinary wing synthesis capability for planform shape as well as sizing type design variables, the designer has to resort to parametric studies.[20,21]

Modern structural synthesis and most efforts in the area of multidisciplinary optimization of complex systems are based on the nonlinear programming/approximation concepts approach (NLP/AC).[22] If optimization routines communicate directly with routines that provide high-fidelity objective function and constraint values for the optimization of complex systems, computational resources become excessive, since computationally expensive analyses have to be performed many times in response to design changes in the evolving system. In NLP/AC, detailed analysis and behavior sensitivity analysis are carried out only a few times during design synthesis. These base designs (or reference designs, as they are sometimes called) are used to construct approximations of the objective function and constraints, and the optimization is carried out using these approximations. Since accuracy of the approximation tends to deteriorate as the design moves away from the base point, additional constraints are added to each approximate optimization problem in the form of move limits on the design variables. Thus, efficient behavior sensitivity evaluation and robust approximations are crucial for effective NLP/AC synthesis. When new disciplines are brought into the framework of multidisciplinary design optimization (MDO), sensitivity and accuracy of the approximations should be evaluated before any optimization attempts are made.

In the structures discipline, derivation of analytic shape sensitivities of mass and stiffness matrices for realistic wing structures and studies of related approximation concepts were reported recently.[23,24] Both finite element and equivalent plate models were used. In linearized unsteady aerodynamics—still used for all practical flutter calculations for airplanes in the subsonic and supersonic speed regimes—progress has been made in the area of sensitivity analysis with lifting line and lifting surface theories.[25,26] The semianalytic method for sensitivity with respect to reduced frequency and Mach number was investigated with lifting surface aerodynamics of fixed planforms,[27] and sensitivities of flutter speed and frequency with respect to planform changes were developed using simple aerodynamics.[28] None of the works just described, however, can address planform sensitivity of complex lifting surface configurations, where multiple lifting surfaces can be involved, including control surfaces for active control.

Moreover, when the aeroservoelastic control design problem is formulated for control system synthesis via methods of modern control theory, a linear time invariant (LTI) mathematical model of the integrated structure, aerodynamics, and control system has to be constructed.[29–31] The generalized aerodynamic forces that are usually evaluated on the imaginary axis of the Laplace plane (for a set of reduced frequencies covering the frequency range of interest) have to be approximated using some rational function expansion in the Laplace variable.[32–34] For integrated aeroservoelastic synthesis, then, sensitivity of these rational function approximations with respect to planform variations has to be available, and effective approximations have to be investigated.

In this paper, several issues concerning modeling, sensitivity calculation, and approximation concepts for aeroservoelastic planform design optimization are discussed. Aeroelastic and aeroservoelastic modeling are reviewed in the context of NLP/AC approach to optimization. Unsteady aerodynamic sensitivity computation for general planar lifting surfaces is discussed. Rational function approximation sensitivity and aeroservoelastic pole sensitivities are studied leading to examination of the performance of different behavior function approximations in the presence of wing and control surface planform changes.

Shape Sensitivity of Unsteady Aerodynamic Forces using Finite Elements and Aerodynamic Lattice Methods

Let the Laplace transformed equations of motion (corresponding to structural degrees of freedom) for an elastic airplane with control surfaces be partitioned as follows:

$$\left\{p^2[M_{ss}] + p[C_{ss}] + [K_{ss}] - q_D[Q_{ss}(p)]\right\}\{q_s(p)\} + \left\{p^2[M_{sc}] - q_D[Q_{sc}(p)]\right\}\{q_c(p)\} = q_D/U\{Q_{sG}\}w_G(p) \quad (1)$$

where w_G is the gust velocity and all other terms are as defined in the nomenclature. With ns structural degrees of freedom, all structural matrices (ss) are of dimension $ns \times ns$. It is assumed, for simplicity, that there is one control surface ($nc = 1$). Thus, the matrices indexed sc are of dimension $ns \times 1$. With a single gust input ($nG = 1$), the aerodynamic matrix indexed sG is of dimension $ns \times 1$.

The structural aeroelastic equations [Eq. (1)] are the basis for flutter analysis (no controls and no gust input), aeroservoelastic stability analysis (no gust input), or dynamic response to atmospheric gusts. They apply to cases where linear structural modeling and linear unsteady aerodynamics provide adequate representation for the aeroelastic behavior of deformable aircraft and have been used successfully for the aeroelastic analysis of airplanes flying in the subsonic and supersonic flight regimes. When detailed finite element structural models are used, the order of the resulting equations is usually reduced by some form of modal approximation.

If the partitioned full order mass and stiffness matrices are $[M_{ss}^F, M_{sc}^F]$, $[K_{ss}^F, 0]$, respectively, and the full order displacement vector is $\{x\}$, then they are replaced by generalized stiffness, mass and a vector of generalized displacements obtained by

$$\{x\} = [\Phi]\{q\} \tag{2}$$

and

$$[K_{ss}] = [\Phi^T]\left[K_{ss}^F\right][\Phi] \tag{3}$$

$$[M_{ss}] = [\Phi^T]\left[M_{ss}^F\right][\Phi] \tag{4}$$

$$[M_{sc}] = [\Phi^T]\left[M_{sc}^F\right] \tag{5}$$

The matrix $[\Phi]$ contains a subset of the normal modes of the nominal structure, or normal modes of the modified structure, or a set of suitable Ritz vectors.[2,31]

Using any aerodynamic panel or lattice method[35] the complex normalized unsteady pressures for simple harmonic motion, due to motion in a given mode shape j, are found from the aerodynamic equations

$$[A(k, M_\infty)]\frac{\{\Delta p^j\}}{8\pi} = \left\{\frac{\partial h^j}{\partial x} + j\frac{k}{b}h^j\right\} \tag{6}$$

where k and M_∞ are the reduced frequency and flight Mach number, respectively. The vector $\{\Delta p^j\}$ contains pressures, and the vectors $\{h^j\}$, $\{(\partial h^j)/(\partial x)\}$ contain displacements and geometric angles of attack (slopes) at the aerodynamic downwash points. The element i, j of the generalized aerodynamic force matrix is then obtained from

$$Q_{ij}(k, M_\infty) = \{h^i\}^T[\Delta S]\{\Delta p^j\} \tag{7}$$

where $[\Delta S]$ is a diagonal matrix of element areas, and $\{h^i\}$ is the vector of modal deflections at the pressure points.

Since the structural mesh and the aerodynamic mesh are usually different, there is a need to interpolate displacements h and slopes $(\partial h)/(\partial x)$ from the structural to the aerodynamic points. This will involve three interpolation operations. From structural nodes to downwash points,

$$\{h^j\} = [T_{hd}]\{\varphi^j\} \tag{8}$$

$$\left\{\frac{\partial h^j}{\partial x}\right\} = [T_{\alpha d}]\{\varphi^j\} \tag{9}$$

and from structural nodes to pressure points

$$\{h^i\} = [T_{hp}]\{\varphi^i\} \tag{10}$$

where $\{\varphi\}$ is a vector of modal displacements.

When an assumed pressure mode method is used for the unsteady aerodynamic problem,[35,36] similar expressions are obtained[2] modified to replace Eq. (10) by a matrix equivalent representing numerical integration over the surface. The unknown vector in Eq. (6) is, in this case, a vector of generalized pressures, representing the contributions of different pressure modes to the overall pressure distribution.

Examination of Eqs. (2–10) reveals the effects of planform changes on the sequence of computational operations. Downwash [on the right-hand side of Eq. (6)] is changing because of the change in structural mode shapes (as a result of the changing mass and stiffness of the wing). When a rigid control surface rotation mode is considered, then, with changes in the shape of the control surface, downwash due to motion in this mode will change too. The influence coefficient matrix $[A(k, M_\infty)]$ is changing with the wing geometry and the resulting change in distances between receiving and sending points. The interpolation matrices in Eqs. (8–10) have to reflect new positions of grid or collocation points on the wing. In the integration for generalized force in Eq. (10), the panel areas and the interpolation matrix also change with variations of the planform shape. The coupling between the aerodynamic problem and the structural order reduction problem is also evident. In the context of planform shape optimization, there is still very little experience with the kind of modes to be used and whether to allow them to vary or to keep them fixed as the structure evolves during optimization.[2]

Shape Sensitivity of Unsteady Aerodynamic Forces using Equivalent Plate Structural Models and Aerodynamic Lattice Methods

A focus of this study is on issues of unsteady aerodynamic load variation with planform shape. To do this, it is desirable to find a structural modeling technique where problems of model-order reduction and structural-to-aerodynamic mesh interpolation can be bypassed and left for subsequent studies. The equivalent plate method offers such an opportunity. Using the equivalent plate approach for wing structural modeling,[37–40] it is possible to study effects of planform changes using full-order models. The method is based on Rayleigh-Ritz approximation using a set of admissible global displacement functions. Since reasonable accuracy can be obtained with 20–40 such functions, modal reduction, although still useful, is not necessary, and full order solutions can be obtained. With continuous Ritz functions defined over wing trapezoidal sections (Fig. 1), the problem of interpolation from structural points to aerodynamic downwash points (as present with the finite element method) is avoided, since displacements $h(x, y)$ and slopes $(\partial h)/(\partial x)$ can be easily found wherever necessary.

When an equivalent plate structural formulation is combined with a lattice-type unsteady aerodynamic method, the generalized forces and their shape sensitivities are obtained as follows. Let the Laplace transformed vertical displacement of a particular lifting surface be

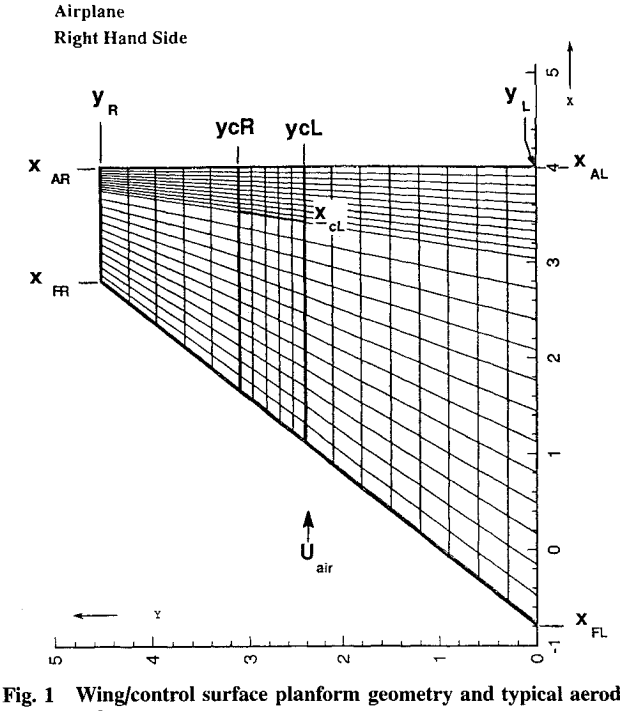

Fig. 1 Wing/control surface planform geometry and typical aerodynamic mesh.

expressed as

$$h(x, y, p) = \sum_{l=1}^{N_q} H_l(x, y) \cdot q_{s_l}(p) + H_c(x, y) q_c(p) \tag{11}$$

where $H_i(x, y)$ is the ith generalized displacement (Ritz function). In the context of polynomial based equivalent plate lifting surface modeling, those Ritz functions are of the form

$$H_i(x, y) = x^{mi} \cdot y^{ni} \tag{12}$$

where mi and ni are powers of x and y, respectively, for the ith polynomial term. In matrix form, focusing on structural degrees of freedom,

$$h(x, y, p) = \left\{H_1(x, y), \ldots, H_{N_q}(x, y)\right\}\{q(p)\} \tag{13}$$

and the vector of displacement at any array of aerodynamic downwash points over the wing can be obtained by

$$\{\boldsymbol{h}\} = \begin{bmatrix} H_1(x_1, y_1) & \cdots & H_{Nq}(x_1, y_1) \\ \cdots & \cdots & \cdots \\ H_1(x_m, y_m) & \cdots & H_{Nq}(x_m, y_m) \end{bmatrix} \{\boldsymbol{q}\} \tag{14}$$

$$\left\{\frac{\partial \boldsymbol{h}}{\partial \boldsymbol{x}}\right\} = \begin{bmatrix} \frac{\partial H_1}{\partial x}(x_1, y_1) & \cdots & \frac{\partial H_{Nq}}{\partial x}(x_1, y_1) \\ \cdots & \cdots & \cdots \\ \frac{\partial H_1}{\partial x}(x_m, y_m) & \cdots & \frac{\partial H_{Nq}}{\partial x}(x_m, y_m) \end{bmatrix} \{\boldsymbol{q}\} \tag{15}$$

The vectors containing slopes and displacements at the downwash points due to motion in the ith Ritz function are given by

$$\left\{\frac{\partial \boldsymbol{H}_i}{\partial \boldsymbol{x}}\right\} = \begin{Bmatrix} \frac{\partial H_i}{\partial x}(x_1, y_1) \\ \cdots \\ \frac{\partial H_i}{\partial x}(x_m, y_m) \end{Bmatrix} \tag{16}$$

and

$$\{\boldsymbol{H}_i\} = \begin{Bmatrix} H_i(x_1, y_1) \\ \cdots \\ H_i(x_m, y_m) \end{Bmatrix} \tag{17}$$

A vector of displacements at the pressure points due to motion in the ith Ritz function is given by

$$\{\tilde{\boldsymbol{H}}_i\} = \begin{Bmatrix} H_i(\tilde{x}_1, \tilde{y}_1) \\ \cdots \\ H_i(\tilde{x}_m, \tilde{y}_m) \end{Bmatrix} \tag{18}$$

When Eq. (6) is solved for the pressures at the pressure points

$$\{\Delta \boldsymbol{p}^j\} = \begin{Bmatrix} \Delta p^j(\tilde{x}_1, \tilde{y}_1) \\ \cdots \\ \Delta p^j(\tilde{x}_m, \tilde{y}_m) \end{Bmatrix} = (8\pi)[A]^{-1} \left\{ \left\{\frac{\partial \boldsymbol{H}_j}{\partial \boldsymbol{x}}\right\} + \hat{j}\frac{k}{b}\{\boldsymbol{H}_j\} \right\} \tag{19}$$

Then, the generalized aerodynamic forces are

$$Q_{ij} = \{\tilde{\boldsymbol{H}}_i\}^T [\Delta S]\{\Delta \boldsymbol{p}^j\} \tag{20}$$

leading to

$$\frac{Q_{ij}}{(8\pi)} = \{\tilde{\boldsymbol{H}}_i\}^T [\Delta S][A]^{-1} \left\{ \left\{\frac{\partial \boldsymbol{H}_j}{\partial \boldsymbol{x}}\right\} + \hat{j}\frac{k}{b}\{\boldsymbol{H}_j\} \right\} \tag{21}$$

Now either an adjoint method or a direct method can be used to obtain the generalized forces. For the adjoint method, a new vector is defined as

$$\{\eta_i\}^* = \{\tilde{\boldsymbol{H}}_i\}^T [\Delta S][A]^{-1} \tag{22}$$

In this case the generalized aerodynamic forces are given by

$$\frac{Q_{ij}}{(8\pi)} = \{\eta_i\}^* \left\{ \left\{\frac{\partial \boldsymbol{H}_j}{\partial \boldsymbol{x}}\right\} + \hat{j}\frac{k}{b}\{\boldsymbol{H}_j\} \right\} \tag{23}$$

where $\{\eta\}$ is the solution of

$$[A]^*\{\eta_i\} = [\Delta S]\{\tilde{\boldsymbol{H}}_i\} \tag{24}$$

Sensitivity with respect to a planform shape design variable (DV) can now be obtained using the adjoint method as follows:

$$[A]^* \frac{\partial\{\eta_i\}}{\partial \mathrm{DV}} = [\Delta S]\frac{\partial\{\tilde{\boldsymbol{H}}_i\}}{\partial \mathrm{DV}} + \frac{\partial[\Delta S]}{\partial \mathrm{DV}}\{\tilde{\boldsymbol{H}}_i\} - \frac{\partial[A]^*}{\partial \mathrm{DV}}\{\eta_i\} \tag{25}$$

so that

$$\frac{1}{(8\pi)}\frac{\partial Q_{ij}}{\partial \mathrm{DV}} = \frac{\partial\{\eta_i\}^*}{\partial \mathrm{DV}} \left\{ \left\{\frac{\partial \boldsymbol{H}_j}{\partial \boldsymbol{x}}\right\} + \hat{j}\frac{k}{b}\{\boldsymbol{H}_j\} \right\} + \{\eta_i\}^* \partial \left\{ \left\{\frac{\partial \boldsymbol{H}_j}{\partial \boldsymbol{x}}\right\} + \hat{j}\frac{k}{b}\{\boldsymbol{H}_j\} \right\} \Big/ \partial \mathrm{DV} \tag{26}$$

When the direct method is used, Eq. (6) is differentiated first to yield

$$\frac{1}{8\pi}[A]\frac{\partial\{\Delta \boldsymbol{p}^j\}}{\partial \mathrm{DV}} = \frac{\partial}{\partial \mathrm{DV}} \left\{ \left\{\frac{\partial \boldsymbol{H}_j}{\partial \boldsymbol{x}}\right\} + \hat{j}\frac{k}{b}\{\boldsymbol{H}_j\} \right\} - \frac{1}{8\pi}\frac{\partial[A]}{\partial \mathrm{DV}}\{\Delta \boldsymbol{p}^j\} \tag{27}$$

which can be solved for $(\partial\{\Delta \boldsymbol{p}^j\})/(\partial \mathrm{DV})$. Then (Eq. 20),

$$\frac{\partial Q_{ij}}{\partial \mathrm{DV}} = \frac{\partial\{\tilde{\boldsymbol{H}}_i\}^T}{\partial \mathrm{DV}}[\Delta S]\{\Delta \boldsymbol{p}^j\} + \{\tilde{\boldsymbol{H}}_i\}^T \frac{\partial}{\partial \mathrm{DV}}\{[\Delta S]\{\Delta \boldsymbol{p}^j\}\} \tag{28}$$

Note that when sensitivities with respect to reduced frequency or Mach number are sought (no planform shape changes) the vector derivatives

$$\frac{\partial\{\tilde{\boldsymbol{H}}_i\}}{\partial k}, \qquad \frac{\partial[\Delta S]}{\partial k}\frac{\partial\{\{(\partial \boldsymbol{H}_j)/(\partial \boldsymbol{x})\}\}}{\partial k}, \qquad \frac{\partial\{\{\boldsymbol{H}_j\}\}}{\partial k}$$

are all zero. Therefore, in this case, using the adjoint method

$$[A]^*\frac{\partial\{\eta_i\}}{\partial k} = -\frac{\partial[A]^*}{\partial k}\{\eta_i\} \tag{29}$$

leading to

$$\frac{1}{8\pi}\frac{\partial Q_{ij}}{\partial k} = \frac{\partial\{\eta_i\}^*}{\partial k} \left\{ \left\{\frac{\partial \boldsymbol{H}_j}{\partial \boldsymbol{x}}\right\} + \hat{j}\frac{k}{b}\{\boldsymbol{H}_j\} \right\} + \{\eta_i\}^* \hat{j}\{\boldsymbol{H}_j\}\frac{1}{b} \tag{30}$$

For generalized aerodynamic terms involving rigid control surface rotations, the computation is identical, except that the displacement field described by $\{\boldsymbol{H}_j\}$ now contains displacements patterns where the control surface rotates about its hinge and the rest of the wing does not move.

Aerodynamic Mesh and its Shape Sensitivities

Since the Ritz functions are defined in global x, y axes (Fig. 1) and are independent of the wing planform, variation of the displacement and slope vectors $\{\boldsymbol{H}_i\}$, $\{(\partial \boldsymbol{H}_i)/(\partial \boldsymbol{x})\}$, and $\{\tilde{\boldsymbol{H}}_i\}$ are only due to changes in position of the downwash and pressure points, as they move with the changing configuration. This sensitivity is easy to obtain analytically, since it involves derivatives of polynomial terms with respect to the x and y coordinates at which they are evaluated. Generally,

$$\frac{\partial}{\partial \mathrm{DV}}\left(x_i^{mi} y_i^{ni}\right) = mi\left(x_i^{mi-1} y_i^{ni}\right)\frac{\partial x_i}{\partial \mathrm{DV}} + ni\left(x_i^{mi} y_i^{ni-1}\right)\frac{\partial y_i}{\partial \mathrm{DV}} \tag{31}$$

The wing planform is divided into trapezoids, as shown in Fig. 1, and the number of aerodynamic cells in the chordwise and spanwise direction is preassigned for each trapezoid. Using coordinates of the vertices of each of the trapezoids as shape design variables, simple, explicit mathematical expressions are obtained for the position of

each pressure point or downwash point in terms of these design variables.

$$x_i = x_i(\mathrm{DV}) \qquad y_i = y_i(\mathrm{DV}) \tag{32}$$

The sensitivity of $\{\boldsymbol{H}_i\}$, $\{(\partial \boldsymbol{H}_i)/(\partial \boldsymbol{x})\}$, and $\{\tilde{\boldsymbol{H}}_i\}$ with respect to planform shape design variables is then obtained by chain rule differentiation.

Analytic Planform Shape Sensitivities with the Doublet Point Method

Among the unsteady aerodynamics lifting surface methods for planar wing configurations, the doublet point method (DPM)[41–43] stands out for its simplicity and ease of implementation. Its accuracy is similar to that of the doublet lattice method for subsonic flows. For supersonic flows, it yields flutter results in good correlation with those obtained by assumed pressure methods or panel methods.[44] It can be applied to general planar configurations with multiple lifting surfaces and control surfaces. Aerodynamic influence coefficients for Eq. (6) are obtained using explicit formulas. The combination of applicability to real airplanes and the simplicity of formulation, made the DPM the method of choice for this exploratory study of unsteady aerodynamic and aeroservoelastic issues for planform shape optimization.

Lumping element pressures and areas together into element forces in DPM, leads to generalized force expressions in the forms:

$$Q_{i,j} = \sum_{l=1}^{m} H_{l,i}\,\Delta p_{l,j} S_l = \sum_{l=1}^{m} H_{l,i} F_{l,j} \tag{33}$$

The sensitivity to design parameter DV is

$$\frac{\partial Q_{i,j}}{\partial \mathrm{DV}} = \sum_{l=1}^{m} \left\{ \frac{\partial H_{l,i}}{\partial \mathrm{DV}} F_{l,j} + H_{l,i} \frac{\partial F_{l,j}}{\partial \mathrm{DV}} \right\} \tag{34}$$

where the force on element l due to motion in generalized displacement j is $F_{l,j} = \Delta p_{l,j}$. In our calculation, the vector $\{\boldsymbol{F}_j\}$ and its derivative $\{(\partial \boldsymbol{F}_j)/(\partial \mathrm{DV})\}$ are obtained as follows.

The lifting surface integral equation relating downwash at point i to pressures on panel j of the aerodynamic mesh is discretized. For some downwash distribution $\{w\}$ and the corresponding aerodynamic forces $\{F\}$ (the double-index notation is now dropped in favor of a single-index notation denoting points on the wing),

$$w_i = \frac{1}{8\pi} \sum_{j=1}^{m} K_{er}[x_i - \xi_j, y_i - \eta_j, k, M_\infty] F_j \tag{35}$$

where the kernel function is given by

$$K_{er}(x_0, y_0, k, M_\infty) = e^{-jkx_0} \left\{ \frac{M e^{jkX}}{R\sqrt{X^2 + y_0^2}} + B(k, y_0, X) \right\} \tag{36}$$

where

$$x_0 = \frac{x_i - \xi_j}{b}, \qquad y_0 = \frac{y_i - \eta_j}{b} \tag{37}$$

$$R = \sqrt{x_0^2 + \beta^2 y_0^2} \tag{38}$$

$$X = (x_0 - M_\infty R)/\beta^2 \tag{39}$$

The function B is given by

$$B(k, y_0, X) = \int_{-\infty}^{X} \frac{e^{\hat{j}kv}}{\left(y_0^2 + v^2\right)^{3/2}}\, \mathrm{d}v \tag{40}$$

References 41 and 42 provide an expansion series formulation for calculating the real and imaginary parts of the B integral

$$B(k, y_0, X) = B_R(k, y_0, X) + \hat{j} B_I(k, y_0, X) \tag{41}$$

The discretized equations [Eq. (35)] can be differentiated

$$\frac{1}{8\pi} \sum_{j=1}^{m} \left\{ \frac{\partial K_{er}}{\partial \mathrm{DV}} F_j + K_{er} \frac{\partial F_j}{\partial \mathrm{DV}} \right\} = \frac{\partial w_i}{\partial \mathrm{DV}} \tag{42}$$

Now, the mesh deforms with the changing planform, and so the downwash at point (x_i, y_i) changes too

$$\frac{\partial w_i}{\partial \mathrm{DV}} = \frac{\partial w_i}{\partial x_i} \frac{\partial x_i}{\partial \mathrm{DV}} + \frac{\partial w_i}{\partial y_i} \frac{\partial y_i}{\partial \mathrm{DV}} \tag{43}$$

The derivative of the kernel term is determined by following changes in the relative positions of sending and receiving points

$$\frac{\partial K_{er}}{\partial \mathrm{DV}} = \frac{\partial K_{er}}{\partial x_0} \frac{\partial x_0}{\partial \mathrm{DV}} + \frac{\partial K_{er}}{\partial y_0} \frac{\partial y_0}{\partial \mathrm{DV}} \tag{44}$$

The expansion in Refs. 41 and 42 for $B(k, y_0, X)$ is used to obtain $(\partial K_{er})/(\partial x_0)$ and $(\partial K_{er})/(\partial y_0)$ explicitly. The force sensitivities $\partial(F_j)/(\partial \mathrm{DV})$ are then found from

$$[K_{er}] \left\{ \frac{\partial F}{\partial \mathrm{DV}} \right\} = 8\pi \left\{ \frac{\partial w}{\partial \mathrm{DV}} \right\} - \left[\frac{\partial K_{er}}{\partial \mathrm{DV}} \right] \{F\} \tag{45}$$

It should be noted that the function $B_R(k, y_0, X)$ has a y_0^{-2} singularity as $y_0 \to 0$ and $X > 0$. After some involved derivation in Ref. 41, to handle sending boxes which are ahead of receiving boxes on the same strip, $B_R(k, y_0, X)$ is replaced by

$$-B_R(k, 0, -X) - \frac{\pi^2}{6\sigma_j^2} + k^2 \left(\ln \frac{k\sigma_j}{2} + \gamma - \frac{3}{2} \right)$$

$$\text{for} \qquad (y_0 < \sigma_j,\ X > 0)$$

where σ_j is the half-width of the jth box. To improve the calculation results for wings with nonuniform strip distribution, Ref. 43 replaces the integral $I_j = -\pi^2/6\sigma_j^2$ with $I_j = -(S_1 + S_2)/2\sigma_j$ where

$$S_1 = \sum_{k=j+1}^{\infty} \frac{2\sigma_k}{\left(y_{k_c} - y_{j_c}\right)^2},$$

$$S_2 = \sum_{k=1}^{j-1} \frac{2\sigma_k}{\left(y_{k_c} - y_{j_c}\right)^2} + \sum_{k=1}^{\infty} \frac{2\sigma_k}{\left(y_{k_c} - y_{j_c}\right)^2} \tag{46}$$

and y_{j_c} and y_{k_c} are y coordinates of the centers of jth and kth strip. The widths of strips beyond the wing tip is assumed equal to that of the last strip on the wing. When there are span variations, as the planform changes shape, care must be taken to take into account the changing widths of the aerodynamic strips and link them to the shape design variables by chain rule differentiation. The sensitivities of the expressions S_1 and S_2 can thus be obtained.

Rational Function Approximations

To model aeroservoelastic systems by linear time invariant state space models, the unsteady generalized loads (which are usually evaluated along the imaginary axis in the Laplace plane for a number of reduced frequencies) have to be approximated by some form of rational function expansion in the Laplace variable p. Several techniques are available for this purpose. The most efficient of them, in terms of the resulting size of the problem (the number of aerodynamic states added) is the minimum state (MS) approach of Refs. 31 and 33. Another element that contributes to the accuracy of the MS method is the physical weighting used, in which weights are assigned to different terms in the generalized aerodynamic force matrix. These weights are determined by examination of the aeroelastic behavior of the open-loop system with its known mass and stiffness distributions.

When it comes to planform shape optimization, where major changes in the planform may occur, two problems arise with the MS method. First, to obtain the MS approximants, an iterative time consuming computation is required. Having to repeat such computations several times in the course of NLP/AC optimization may be

impractical. The iterative nature of the process also makes it difficult to calculate shape sensitivities of the resulting approximants. In addition, having to use physical weighting for a system whose dynamic characteristics are not known in advance, and are changing continuously, is also a challenge.

Research is currently directed at resolving these problems. For the current study, however, the Roger approximation method[32] is selected, because of its simplicity and ease of obtaining analytic sensitivities with respect to planform shape variables. The Roger approximation is of the form

$$[Q(\hat{jk})] \approx [E_0]+(\hat{jk})[E_1]+(\hat{jk})^2[E_2]+\sum_{l=1}^{m_L}\frac{\hat{jk}}{\hat{jk}+\beta_l}[E_{l+2}] \quad (47)$$

where the matrices $[E_j]$ and the lag terms β_l are real. The approximation is forced to match the exact data at $k = 0$. Separating to real and imaginary parts

$$\mathrm{Re}[Q(\hat{jk})] \approx [E_0] - k^2[E_2] + \sum_{l=1}^{m_L}\frac{k^2}{k^2+\beta_l^2}[E_{l+2}] \quad (48)$$

$$\mathrm{Im}[Q(\hat{jk})] \approx k[E_1] + \sum_{l=1}^{m_L}\frac{k\beta_l}{k^2+\beta_l^2}[E_{l+2}] \quad (49)$$

The approximation is carried out in a least square manner term by term to determine elements of the $[E_i]$ matrices. The lag roots β_l are the same for all elements of the generalized aerodynamic matrix. They can be optimized, but this will just add to the computational cost of overall aeroservoelastic shape optimization, and is not considered necessary at this stage.

Focusing on the element i, j of the aerodynamic matrix and its Roger matrices elements $e0, e1, e2, \ldots$, we have for that element evaluated at $nk + 1$ reduced frequencies (including $k = 0$)

$$\begin{bmatrix} 0 & -(k1)^2 & \frac{(k1^2)}{(k1^2+\beta 1^2)} & \cdots \\ k1 & 0 & \frac{k1\beta 1}{(k1^2+\beta 1^2)} & \cdots \\ 0 & -(k2)^2 & \frac{(k2^2)}{(k2^2+\beta 1^2)} & \cdots \\ k2 & 0 & \frac{k2\beta 1}{(k2^2+\beta 1^2)} & \cdots \\ \cdots & \cdots & \cdots & \cdots \end{bmatrix} \begin{Bmatrix} e_1 \\ e_2 \\ e_3 \\ \cdots \\ \cdots \end{Bmatrix}$$

$$= \begin{Bmatrix} Q_{R,ij}(k1) - Q_{R,ij}(0) \\ Q_{I,ij}(k1) \\ Q_{R,ij}(k2) - Q_{R,ij}(0) \\ Q_{I,ij}(k2) \\ \cdots \end{Bmatrix} \quad (50)$$

This can be written in the form

$$[L]\{e\} \approx \{\boldsymbol{R}\}$$

and for a least square solution

$$[L]^T[L]\{e\} = [L]^T\{\boldsymbol{R}\} \quad (51)$$

In Eqs. (50) and (51) we can see that the vector $\{\boldsymbol{R}\}$ on the right-hand side changes with variations in planform shape, due to changes in the generalized loads. The matrix $[L]$ depends only on the lag roots and the values of reduced frequencies at which unsteady aerodynamic forces are available. The shape sensitivity of the $[E]$ matrices of the Roger approximation, then, are determined term by term from

$$[L]^T[L]\left\{\frac{\partial e}{\partial \mathrm{DV}}\right\} = [L]^T\left\{\frac{\partial \boldsymbol{R}}{\partial \mathrm{DV}}\right\} \quad (52)$$

Thus, based on the sensitivities of generalized forces, the sensitivities $(\partial[E_1])/(\partial \mathrm{DV})$, $(\partial[E_2])/(\partial \mathrm{DV})$, $(\partial[E_3])/(\partial \mathrm{DV}), \ldots$ are found. The shape sensitivity of E_0 is obtained directly from the sensitivity of the steady-state generalized force matrix ($k = 0$). Note that if constraints are imposed on the approximation (to force it to match the real and imaginary parts of the Q_{ij} term exactly at a second reduced frequency kf, for example) the equations have to be modified, the matrices $[E1]$ and $[E2]$ are eliminated and expressed in terms of $[E3]$, $[E4]$, etc., but the equations for sensitivity of the resulting Roger matrices are of the same form as Eqs. (51) and (52).

Aeroservoelastic Models and their Planform Shape Sensitivity

For simplicity we focus on aeroservoelastic stability in this study, and the gust excitation terms are dropped out. Furthermore, since the emphasis here is on effects of variation in mass, stiffness, and aerodynamic matrices due to planform shape changes, no control system is modeled. Detailed derivations of the aeroservoelastic equations in the presence of an active control system can be found elsewhere (Refs. 29–31). Here we close the loop by a simple deformation (displacement or angle of attack) feedback control law

$$q_c = [G]\{\boldsymbol{q}_s\} \quad (53)$$

The matrix $[G]$ depends on the location $(\bar{x}, \bar{y})$ at which displacement is measured and a gain Γ.

$$q_c = G\{\boldsymbol{q}_s\} = \Gamma\{\boldsymbol{H}_1(\bar{x}, \bar{y}), \ldots, \boldsymbol{H}_i(\bar{x}, \bar{y}), \ldots, \ldots\}\{\boldsymbol{q}_s\} \quad (54)$$

Using the Roger series to replace the generalized aerodynamic forces $[Q_{ss}, Q_{sc}]$ and the control law [Eq. (53)] to eliminate q_c, the following equations are obtained based on Eq. (1):

$$[\hat{M}_{ss} + \hat{M}_{sc}G]p^2\{\boldsymbol{q}_s\} + [\hat{C}_{ss} + \hat{C}_{sc}G]p\{\boldsymbol{q}_s\} + [\hat{K}_{ss} + \hat{K}_{sc}G]\{\boldsymbol{q}_s\} - q_D[A_{3ss} + A_{3sc}G] \times \frac{p}{p+\hat{\beta}_1}\{\boldsymbol{q}_s\} - \cdots = 0 \quad (55)$$

where

$$[\hat{M}_{ss}] = [M_{ss}] - q_D(b^2/U^2)[A_{2ss}] \quad (56)$$

$$[\hat{C}_{ss}] = [C_{ss}] - q_D(b/U)[A_{1ss}] \quad (57)$$

$$[\hat{K}_{ss}] = [K_{ss}] - q_D[A_{0ss}] \quad (58)$$

$$[\hat{M}_{sc}] = [M_{sc}] - q_D(b^2/U^2)[A_{2sc}] \quad (59)$$

$$[\hat{C}_{sc}] = -q_D(b/U)[A_{1sc}] \quad (60)$$

$$[\hat{K}_{sc}] = -q_D[A_{0sc}] \quad (61)$$

$$\hat{\beta}_i = \beta_i(U/b) \quad (62)$$

State variables are now introduced as follows:

$$\{\boldsymbol{x}1\} = \{\boldsymbol{q}_s\} \quad (63)$$

$$\{\boldsymbol{x}2\} = p\{\boldsymbol{q}_s\} \quad (64)$$

$$\{\boldsymbol{x}3\} = \sqrt{q_D}\frac{p}{p+\hat{\beta}_1}\{\boldsymbol{q}_s\} \quad (65)$$

$$\{\boldsymbol{x}4\} = \sqrt{q_D}\frac{p}{p+\hat{\beta}_2}\{\boldsymbol{q}_s\} \quad (66)$$

and so on, depending on the number of lag terms used in the Roger approximation. The resulting state space equations for the closed loop system are, then,

$$p[U]\{\boldsymbol{x}\} = [V]\{\boldsymbol{x}\} \quad (67)$$

where $\{\boldsymbol{x}\}^T = \{\boldsymbol{x}1^T, \boldsymbol{x}2^T, \boldsymbol{x}3^T, \boldsymbol{x}4^T, \ldots\}$ is the state vector contain-

ing structural and aerodynamic states. The matrices in Eq. (67) are given by

$$[U] = \begin{bmatrix} [I] & 0 & 0 & 0 \\ 0 & [\hat{M}_{ss} + \hat{M}_{sc}G] & 0 & 0 \\ 0 & 0 & [I] & 0 \\ 0 & 0 & 0 & \dots \end{bmatrix} \tag{68}$$

and

$$[V] = \begin{bmatrix} 0 & [I] & 0 & 0 \\ -[\hat{K}_{ss} + \hat{K}_{sc}G] & -[\hat{C}_{ss} + \hat{C}_{sc}G] & \sqrt{q_D}[A_{3ss} + A_{3sc}G] & \cdots \\ 0 & \sqrt{q_D}[I] & -\hat{\beta}_1[I] & 0 \\ 0 & \cdots & 0 & \dots \end{bmatrix} \tag{69}$$

The effects of structural and aerodynamic changes due to planform shape variations can now be studied. The $[U]$ and $[V]$ matrices are linear in stiffness, mass, and aerodynamic Roger terms. The control law introduces coupling between structural and aerodynamic terms. The matrix G depends on planform shape and on the location of the measurement point on the wing. Thus with planform changes, this matrix will change too.

By using analytic shape sensitivities of the full-order stiffness and mass matrices[24] together with the analytic shape sensitivities of the Roger matrices [Eq. (52)], and coupled with the easily obtained analytic sensitivity of the matrix $[G]$ [Eq. (54)] when a control law is present, the sensitivities of $[U]$ and $[V]$ can be obtained analytically with respect to planform shape. The sensitivity of aeroservoelastic poles can now be calculated by

$$\frac{\partial \lambda}{\partial \mathrm{DV}} = \left[\left(\{\psi\}^T \left[\lambda \frac{\partial U}{\partial \mathrm{DV}} - \frac{\partial V}{\partial \mathrm{DV}} \right] \{\theta\} \right) \Big/ \left(\{\psi\}^T [U] \{\theta\} \right) \right] \tag{70}$$

where λ is a pole, and $\{\theta\}$ and $\{\psi\}$ are right and left eigenvectors, respectively.

Aeroservoelastic Pole Approximations

Several approximation techniques for aeroservoelastic poles should now be considered. Taylor series based approximations in direct design variables or reciprocal design variables[45] can be based on the pole derivatives [Eq. (70)]. If the real and imaginary parts of the poles are considered

$$\lambda = \sigma + \hat{j}\omega \tag{71}$$

then their Taylor series approximations can be used in the equation for the damping ratio

$$\zeta = \frac{\sigma}{\sqrt{\sigma^2 + \omega^2}} \tag{72}$$

Alternatively, a Rayleigh quotient approximation (RQA) can be constructed,[46–48] in which the derivatives of the matrices $[U]$ and $[V]$ are used

$$\lambda = \frac{\{\psi\}^T [\tilde{V}(\mathrm{DV})] \{\theta\}}{\{\psi\}^T [\tilde{U}(\mathrm{DV})] \{\theta\}} \tag{73}$$

Direct or reciprocal Taylor series approximations can be used for the approximate $[U]$ and $[V]$, assuming that the left and right eigenvectors do not change and are fixed at their values at the base design.

It is important to emphasize, in this context, the computationally intensive nature of computing unsteady aerodynamic forces. Not only is it time consuming to assemble the influence coefficient matrix and solve Eq. (6), this has to be done at many reduced frequencies, for the least squares fitting process which will generate the Roger approximation matrices.

Experience with aeroservoelastic pole approximations to date has shown that it is necessary to use very narrow move limits because of the highly nonlinear nature of these poles.[13,14,48] A major source of error in either the Taylor series approximations or RQAs comes from the fact that whereas the system matrices are changed, the eigenproblem is not solved again with the new matrices. Now, in the case of sizing-type structural design variables and fixed planforms, the full-order system matrices $[U]$ and $[V]$ are linear in the design variables. If Taylor series approximations in direct design variables are used for those matrices, the approximate $[U]$ and $[V]$ will be identical to the exact ones. If, then, approximate matrices were used, but the eigenvalue problem solved completely, the exact eigenvalues would be recovered.

In the case of planform shape variations, it is tempting to examine aeroservoelastic poles obtained by full eigenvalue analysis of the system but with approximated system matrices. Even with relatively large aeroservoelastic models (say, 60–100 states) still a complete eigensolution can be quite fast, whereas the number of detailed computations of the unsteady aerodynamic matrices should be kept to a minimum. One form of approximation, then, that will be used here to study effects of errors in mass, stiffness, and aerodynamic approximations on the errors in aeroservoelastic poles, will involve full eigenvalue solution of the generalized eigenvalue problem

$$\lambda[\tilde{U}]\{x\} = [\tilde{V}]\{x\} \tag{74}$$

where $[\tilde{U}]$, $[\tilde{V}]$ are approximated system matrices based on either direct or reciprocal Taylor series expansions.

For effective aeroservoelastic optimization with planform changes, it is also important to consider using a smaller number of lag terms in the Roger series (to reduce the resulting size of the aeroservoelastic model) and a smaller number of reduced frequencies for the least square rational function series fitting. Compared with other sources of error in the approximations used, certain inaccuracies due to fewer lag terms and fewer reduced frequencies may be tolerated, and the computational gain, at the same time, can be significant. Quantitative evaluation of accuracy and efficiency with fewer lag terms and reduced frequencies is beyond the scope of this article.

Test Case

A fighter-type wing was used for numerical studies. It is an all aluminum wing and has, in addition to cover skins, six spars uniformly distributed chordwise, and 11 ribs uniformly distributed spanwise. A 3.5% t/c parabolic airfoil was used. The wing has a half-span (Y_R) of 4.5 m, a root chord of 4.8 m, and a tip chord of 1.2 m, as shown in Fig. 1. A small 20% chord control surface is placed between $y = 2.4$ and $y = 3.1$ m. Skin thickness over the wing is 0.00509 m, spar and rib cap areas are 0.00006 m^2. Two torsion springs at the right and left sides of the control surface connect it to the wing box. Their stiffness coefficient is 10^5 N-m/rad. The ideal structural weight of the wing is 403.33 Kg. An additional 403.33 Kg of nonstructural weight is distributed uniformly over the wing. In addition, an 80-Kg wing tip pod is simulated by concentrated masses attached to the wing tip, with a center of mass at 28.75% of the tip chord. Planform variations in the form of span changes (Y_R, keeping a fixed tip chord), and leading-edge sweep changes (due to motion of the forward tip point in the x direction, X_{FR}) were studied, in addition to changes in size and location of the trailing-edge control surface.

The displacement Ritz series used for structural analysis was a complete polynomial with terms up to y^5. The wing was cantilevered at the root. When no control surface was present, the generalized unsteady aerodynamic force matrices were of order 21 × 21. When the control surface was present, six polynomial terms (a complete quadratic) were used for control surface deformation in addition to its rigid rotation with respect to the hinge line. The unsteady aerodynamic forces were calculated at a Mach number of 0.8, and sea level standard atmospheric conditions were used in the aeroservoelastic stability analysis. The DPM mesh used for aerodynamic computations for the wing with control surface is shown in Fig. 1. For the wing without control surface, a uniform mesh of 20 × 20 was used. When Roger approximation were constructed, four lag terms were used to fit aerodynamic matrices calculated at 15 reduced frequencies covering the range 0–2. No attempt was made to optimize the lag terms themselves, and they were fixed at 0.5, 1.0, 1.5, and 2.0. All aerodynamic computations were done on a DEC 5000/200 workstation.

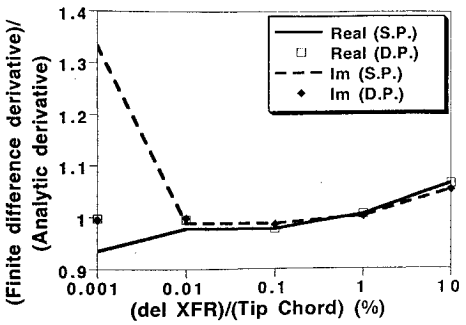

Fig. 2 Accuracy of finite difference generalized aerodynamic force sentivity with respect to X_{FR} for the Ritz function $x^2y^2(q_{13})$, single and double precision.

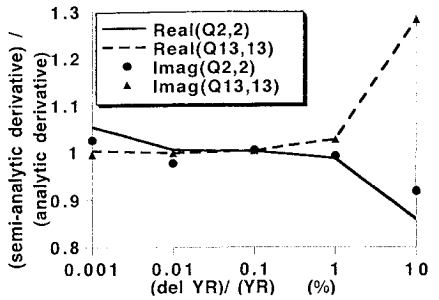

Fig. 3 Accuracy of semianalytic generalized aerodynamic force sentivity with respect to span Y_R for the Ritz functions $x(q_2)$ and $x^2y^2(q_{13})$, single precision.

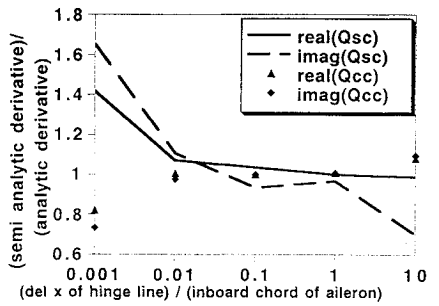

Fig. 4 Accuracy of semianalytic generalized aerodynamic force sentivity with respect to control surface root chord x_{CL}, structural Ritz function $x^2y^2(q_s)$ over the wing box, control surface rotation q_c, single precision.

Results

Both finite difference and semianalytic derivatives can be quite sensitive to the step size chosen,[45] and this sensitivity is problem dependent. With analytic shape sensitivities now available for the unsteady aerodynamic forces, the accuracy of corresponding finite difference and semianalytic sensitivity computations, and the effect of step size, can be assessed. Figure 2 shows the effect of step size on the finite difference derivative of an element of the unsteady aerodynamic force matrix ($Q_{13,13}$, corresponding to Ritz function x^2y^2). Figure 3 shows the effect of step size on semianalytic derivatives of two generalized aerodynamic terms, $Q_{2,2}$ (corresponding to Ritz function x, a pitching motion) and $Q_{13,13}$ for the wing box. For the case when the control surface is present, typical semianalytic sensitivities of aerodynamic terms associated with coupling of control and structural motions (sc) and control dependent terms (cc) are shown in Fig. 4. In all cases there is a wide range of step sizes that will lead to good finite difference or semianalytic derivatives. This is also true for single-precision calculations. It was found that the single-precision aerodynamic results for the force terms are almost identical to the double-precision results. Computer storage space can, then, be reduced without any significant loss in accuracy using single precision for the current problem, even when finite difference or semianalytic sensitivities are required. Moreover, the assembly of the aerodynamic influence coefficient matrix [Eq. (6)] in DPM is very fast compared with other lifting surface methods. Most of the computation time is spent on the solution of Eq. (6) when the number of panels is large. Based on the high reliability of semianalytic results, as shown in Figs. 3 and 4, the semianalytic method with DPM aerodynamics becomes quite attractive.

In Fig. 5, the accuracy of aerodynamic force approximations based on reference data (Y_R = 4.5 m) and shape sensitivities at that base design is examined. Approximate Roger series based on direct Taylor series extrapolation are shown and compared to exact data for various configurations, with Y_R changing from 3.5 m to 5.5 m, the extrapolated values are quite accurate. Different terms of the unsteady aerodynamic matrix behave in a similar manner, and in some cases the approximation seems to perform well for relatively far values of Y_R. Overall approximation error[31] averaging the fitting errors for all terms over all reduced frequencies are shown in Fig. 6.

Attention is turned next to effects of errors in aerodynamic terms and structural terms on aeroservoelastic pole approximations. The results shown in Fig. 7 were obtained by full eigenvalue analysis. Damping ratios for the first bending mode (wing only) are compared for the case where all structural and aerodynamic matrices are exact, the case where the mass and stiffness matrices are exact

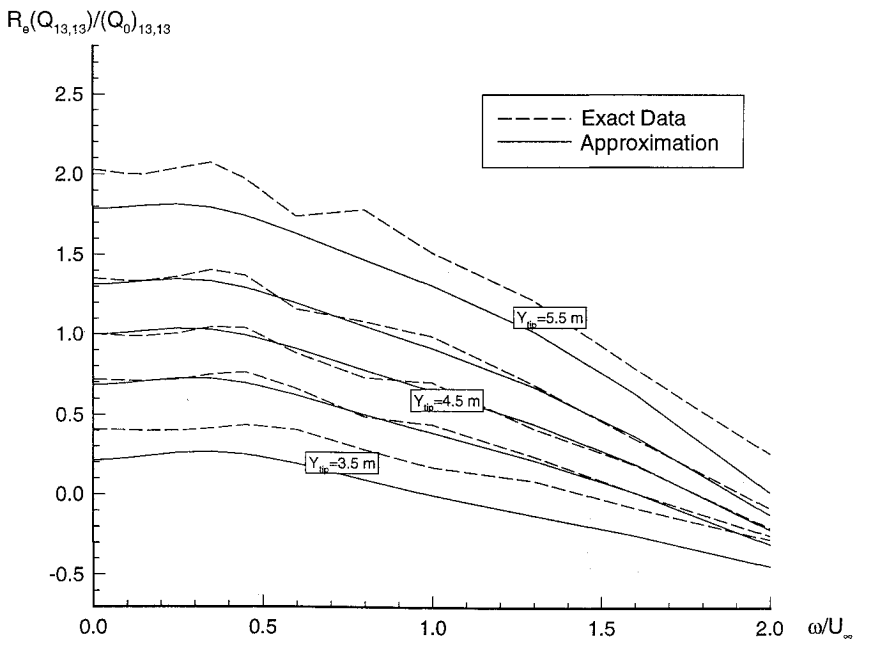

Fig. 5 Direct Taylor series approximation for generalized force $Q_{13,13}$ with semispan variations.

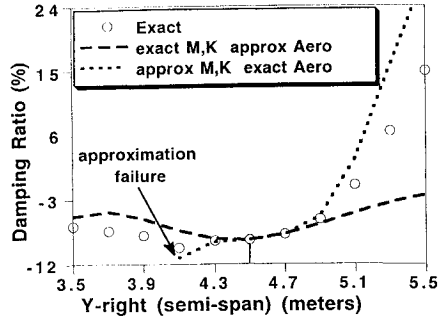

Fig. 6 Total approximation error for direct Taylor approximation of the generalized aerodynamic force matrix.

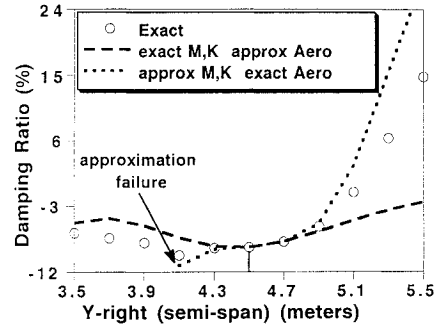

Fig. 7 Damping ratio approximations for the first bending mode: full eigenvalue analysis, wing without control surface.

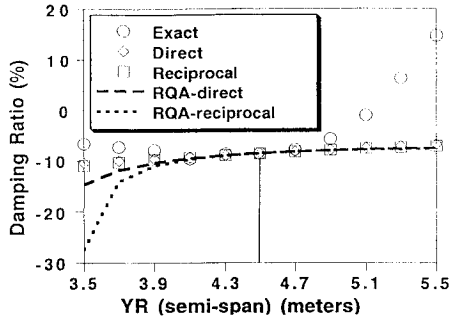

Fig. 8 Damping ratio approximations for the first bending mode: Taylor series and Rayleigh quotient approximations, wing without control surface.

although aerodynamic terms are approximated, and the case where aerodynamic terms are exact and mass and stiffness terms are approximated. Direct Taylor approximations are shown. As the figure shows, move limits of only about 5% can be allowed for reasonable accuracy. Also notice the sensitivity of the approximation to errors in the mass and stiffness terms. Even with mild shape changes, away from the base design, the approximated M and K matrices may lead to large errors in the aeroservoelastic poles, often correlated with errors in the natural frequencies of the approximated structure. Taylor series and Rayleigh quotient approximations for the complex eigenvalues directly (Fig. 8) do not fail away from the base point (as the approximation in Fig. 7). They, too, are only accurate within about 5% move limits and do not capture the correct curvature of the damping ratio curve for this root. Similar results were obtained for the first bending frequency and for other modes.

When a control surface is activated by a wing tip angle of attack feedback (with a gain of 2.5), aeroservoelastic poles move when the control surface shape and position change. Results for the case when the right-hand side of the control surface moves from $y_{cR} = 2.7$ to $y_{cR} = 3.5$ m are shown in Fig. 9. Approximations of the damping ratio of a typical pole are based on aerodynamic and structural matrices and their shape sensitivity at $y_{cR} = 3.1$ m. Full eigenvalue analysis with the approximate matrices is used. Again, the limitations due to mass and stiffness extrapolation errors is evident. In this case, when

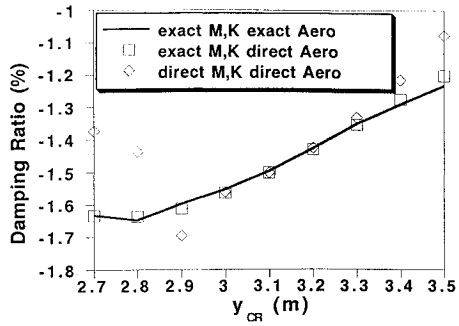

Fig. 9 Damping ratio approximations for the first bending mode, full eigenvalue analysis, actively controlled wing, direct tip angle-of-attack feedback.

aerodynamic approximations are used with exact stiffness and mass matrices, the resulting pole approximation is excellent.

As in the case of aeroservoelastic poles in the presence of an active control system[48] approximation accuracy is problem dependent and may vary when different design variables are involved. Generally, current approximation techniques provide satisfactory information only within small move limits (5% and less) when planform shape is involved.

Conclusions

Equivalent plate structural modeling and doublet point lifting surface unsteady aerodynamics were used to obtain analytic sensitivities of aeroelastic and aeroservoelastic response with respect to wing and control surface planform shape parameters. Rational function approximations for unsteady aerodynamic forces, their shape sensitivities, and the resulting linear time invariant state space models of aeroservoelastic systems and their shape sensitivities were examined. The goal was to develop effective and numerically efficient approximation techniques for wing shape optimization for use with nonlinear programming and approximation concepts as a multidisciplinary optimization strategy. With analytic shape sensitivities available for unsteady aerodynamic loads, it became possible to evaluate the accuracy of finite difference and semianalytic aerodynamic shape sensitivities. It was shown that a wide range of step sizes could be used for obtaining accurate aerodynamic shape sensitivities by the semianalytic and finite difference methods, whether single precision or double precision was used. This is in contrast to the limited range of acceptable step sizes needed for finite difference or semianalytic sensitivity computation with structural equivalent plate models. Effects of structural and unsteady aerodynamic modeling errors were studied in an examination of approximation accuracy using alternative approximation techniques. A new approximation technique for aeroservoelastic poles was presented, in which approximated system matrices are used, but complete eigenanalysis is carried out. For this new approximation, as well as Taylor series based and Rayleigh quotient approximations, it was found that acceptable accuracy could be obtained only within about 5% move limits, due to difficulty in approximating the stiffness, mass, and aerodynamic matrices for large shape variations. These results provide insight and experience and call for additional research on the way to realistic wing/control surface shape optimization with active controls and aeroservoelastic constraints.

Acknowledgment

Support from the National Science Foundation through a National Young Investigator Award is gratefully acknowledged.

References

[1]Haftka, R. T., "Structural Optimization with Aeroelastic Constraints: A Survey of US Applications," *International Journal of Vehicle Design*, Vol. 7, No. 3–4, 1986, pp. 381–392.

[2]Haftka, R. T., and Yates, C. E., Jr., "On Repetitive Flutter Calculations in Structural Design," *Journal of Aircraft*, Vol. 13, No. 7, 1976, pp. 454–461.

[3]Miura, H., and Neill, D. J., "Applications to Fixed-Wing Aircraft and Spacecraft," *Structural Optimization: Status and Promise*, Progress in Astronautics and Aeronautics, edited by M. P. Kamat, AIAA, Washington, DC, 1993, pp. 705–742.

[4]Grossman, B., Gurdal, Z., Strauch, G. J., Eppard, W. M., and Haftka, R. T., "Integrated Aerodynamic/Structural Design of a Sailplane Wing," *Journal of Aircraft*, Vol. 25, No. 9, 1988, pp. 855–860.

[5]Rais-Rohani, M., Haftka, R. T., Grossman, B. M., and Unger, E. R., "Integrated Aerodynamic-Structural-Control Wing Design," *Computing Systems in Engineering*, Vol. 3, No. 6, 1992, pp. 639–650.

[6]Barthelemy, J.-F. M., and Bergen, F. D., "Shape Sensitivity Analysis of Wing Static Aeroelastic Characteristics," NASA TP-2808, May 1988.

[7]Kapania, R. K., Eldred, L. B., and Barthelemy, J.-F. M., "Sensitivity Analysis of a Wing Aeroelastic Response," *Journal of Aircraft*, Vol. 30, No. 4, 1993, pp. 496–504.

[8]Felt, L. R., Huttsell, J., et al., "Aeroservoelastic Encounters," *Journal of Aircraft*, Vol. 16, No. 7, 1979, pp. 477–483.

[9]Becker, J., Weiss, F., and Sensburg, O., "Compatibility Aspects of Active Control Technologies with Aircraft Structural Design," *Structural Control*, edited by H. H. E., Leipholz, Martinus Nijhoff, Dordrecht, the Netherlands, 1987.

[10]Noll, T., Austin, E., Donely, S., Graham, G., Harris, T., Kaynes, I., Lee, B., and Sparrow, J., "Impact of Active Controls Technology on Structural Integrity," *Proceedings of the AIAA/ASCE/ASME/AHS/ASC 32nd Structures, Structural Dynamics, and Materials Conference*, AIAA, Washington, DC, 1991, pp. 1869–1878 (AIAA 91-0988).

[11]Morris, S., and Kroo, I., "Aircraft Design Optimization with Multidisciplinary Performance Criteria," AIAA Paper 89-1265, April 1989.

[12]Bindolino, G., Lanz, M., Mantegazza, P., and Ricci, S., "Integrated Structural Optimization in the Preliminary Aircraft Design," *17th Congress of the International Council of the Aeronautical Sciences* (Stockholm, Sweden), Sept. 1990, pp. 1366–1378 (ICAS-90-5.7.3).

[13]Livne, E., Schmit, L. A., and Friedmann, P. P., "Exploratory Design Studies Using an Integrated Multidisciplinary Synthesis Capability for Actively Controlled Composite Wings," *AIAA Journal*, Vol. 30, No. 5, 1992, pp. 1171–1179.

[14]Livne, E., Friedmann, P. P., and Schmit, L. A., "Integrated Aeroservoelastic Wing Synthesis by Nonlinear Programming/Approximation Concepts," *Journal of Guidance, Control, and Dynamics*, Vol. 15, No. 4, 1992, pp. 985–993.

[15]Karpel, M., "Multidisciplinary Optimization of Aeroservoelastic Systems Using Reduced Size Models," *Journal of Aircraft*, Vol. 29, No. 5, 1992, pp. 939–946.

[16]Sensburg, O., and Laschka, B., "Flutter Induced by Aerodynamic Interference Between Wing and Tail," *Journal of Aircraft*, Vol. 7, July–Aug. 1970, pp. 319–324.

[17]Johnson, T. L., Athans, M., and Skelton, G. B. "Optimal Control Surface Locations for Flexible Aircraft," *Transactions on Automatic Control*, Vol. AC-16, No. 4, 1971, pp. 320–330.

[18]Weisshaar, T. A., and Nam, C., "Aeroservoelastic Tailoring for Lateral Control Enhancement," *Journal of Guidance, Control, and Dynamics*, Vol. 13, No. 3, 1990, pp. 458–467.

[19]Nissim, E., and Burken, J. J., "Control Surface Spanwise Placement in Active Flutter Suppression Systems," *Recent Advances in Multidisciplinary Analysis and Optimization*, NASA Conf. Pub. 3031, edited by F.-F. M. Barthelemy, 1989, pp. 919–934.

[20]Sensburg, O., Schmidinger, G., and Fullhas, K., "Integrated Design of Structures," *Journal of Aircraft*, Vol. 26, No. 3, 1989, pp. 260–270.

[21]Nissim, E., Caspi, A., and Lottati, I., "Application of the Aerodynamic Energy Concept to Flutter Suppression and Gust Alleviation by Use of Aerodynamic Energy," NASA TN D-8212, 1976.

[22]Schmit, L. A., "Structural Optimization—Some Key Ideas and Insights," *New Directions in Optimum Structural Design*, edited by E. Atrek, R. H. Gallagher, K. M. Ragsdell, and O. C. Zienkiewicz, John Wiley, New York, 1984.

[23]Harvey, M., "Design Oriented Finite Element Structural Modeling for Wing Planform Shape Optimization," M.Sc. Thesis, Dept. of Aeronautics and Astronautics, Univ. of Washington, Seattle, WA, 1993.

[24]Livne, E., "Analytic Sensitivities for Shape Optimization in Equivalent Plate Structural Wing Models," *Journal of Aircraft*, Vol. 31, No. 4, 1994, pp. 961–969.

[25]Yates, E. C., Jr., "Aerodynamic Sensitivities from Subsonic, Sonic and Supersonic Unsteady, Nonplanar Lifting Surface Theory," NASA TM 100502, Sept. 1987.

[26]Yates, E. C., "Integral Equation Methods in Steady and Unsteady Subsonic, Transonic and Supersonic Aerodynamics for Interdisciplinary Design," NASA TM 102677, May 1990.

[27]Murthy, D. V., and Kaza, R. V., "Semianalytical Techniques for Sensitivity Analysis of Unsteady Aerodynamic Computations," *Journal of Aircraft*, Vol. 28, Aug. 1991, pp. 481–488.

[28]Kapania, R., Bergen, F., and Barthelemy, J., "Shape Sensitivity Analysis of Flutter Response of a Laminated Wing," AIAA Paper 89-1267, April 1989.

[29]Mukhopadhyay, V., Newsom, J. R., and Abel, I., "A Method for Obtaining Reduced Order Control Laws for High Order Systems Using Optimization Techniques," NASA TP-1876, 1981.

[30]Livne, E., Schmit, L. A., and Friedmann, P. P., "Towards an Integrated Approach to the Optimum Design of Actively Controlled Composite Wings," *Journal of Aircraft*, Vol. 27, Dec. 1990, pp. 979–992.

[31]Karpel, M., "Size Reduction Techniques for the Determination of Efficient Aeroservoelastic Models," *Control and Dynamic Systems—Advances in Theory and Applications*, Vol. 54, Academic Press, 1992, pp. 263–295.

[32]Roger, K. L., "Airplane Math Modeling Methods for Active Control Design," *Structural Aspects of Active Controls*, AGARD CP-228, Aug. 1977, pp. 4–11.

[33]Karpel, M., "Time Domain Aeroservoelastic Modeling Using Weighted Unsteady Aerodynamic Forces," *Journal of Guidance, Control, and Dynamics*, Vol. 13, No. 1, 1990, pp. 30–37.

[34]Eversman, W., and Tewari, A., "Consistent Rational Function Approximation for Unsteady Aerodynamics," *Journal of Aircraft*, Vol. 28, No. 9, 1991, pp. 545–551.

[35]Rowe, W. S., "Comparison of Analysis Methods used in Lifting Surface Theory," *Computational Methods in Potential Aerodynamics*, edited by L. Morino, Springer-Verlag, 1985.

[36]Lottati, I., and Nissim, E., "Three Dimensional Oscillatory Piecewise Continuous Kernel Function Method—Parts I–III, *Journal of Aircraft*, May 1981, pp. 346–363.

[37]Giles, G. L., "Equivalent Plate Analysis of Aircraft Wing Box Structures with General Planform Geometry," *Journal of Aircraft*, Vol. 23, No. 11, 1986, pp. 859–864.

[38]Giles, G. L., "Further Generalization of an Equivalent Plate Representation for Aircraft Structural Analysis," *Journal of Aircraft*, Vol. 26, No. 1, 1989, pp. 67–74.

[39]Livne, E., Sels, R. E., and Bhatia, K. G., "Lessons from Application of Equivalent Plate Structural Modeling to an HSCT Wing," *Journal of Aircraft*, Vol. 31, No. 4, 1994, pp. 953–960.

[40]Livne, E., "Equivalent Plate Structural Modeling for Wing Shape Optimization Including Transverse Shear," *AIAA Journal*, Vol. 32, No. 6, 1994, pp. 1278–1288.

[41]Ueda, T., and Dowell, E. H., "A New Solution Method for Lifting Surfaces in Subsonic Flow," *AIAA Journal*, Vol. 20, No. 3, 1982, pp. 348–355.

[42]Ueda, T., "Expansion Series of Integral Functions Occuring in Unsteady Aerodynamics," *Journal of Aircraft*, Vol. 19, No. 4, 1982, pp. 345–347.

[43]Eversman, W., and Pitt, D. M., "Hybrid Doublet Lattice/Doublet Point Method for Lifting Surfaces in Subsonic Flow," *Journal of Aircraft*, Sept. 1991, pp. 572–578.

[44]Yurkovich, R., private communication, McDonnel Douglas, St. Louis, MO, 1993.

[45]Haftka, R. T., and Gurdal, Z., "Elements of Structural Optimization," 3rd ed., Martinus Nijhoff, Dordrecht, The Netherlands, 1992.

[46]Canfield, R. A., "Design of Frames Against Buckling Using a Rayleigh Quotient Approximation," *AIAA Journal*, Vol. 31, No. 6, 1993, pp. 1144–1149.

[47]Thomas, H. L., and Schmit, L. A., "Improved Approximations for Control Augmented Structural Synthesis," *Proceedings of the AIAA/ASCE/ASME/AHS 31st Structures, Structural Dynamics, and Materials Conference*, Vol. 1, AIAA, Washington, DC, 1990, pp. 277–294.

[48]Livne, E., "Alternative Approximations for Integrated Control/Structure Aeroservoelastic Synthesis," *AIAA Journal*, Vol. 31, No. 6, 1993, pp. 1100–1108.